

No-Reference Quality Assessment for 3D Colored Point Cloud and Mesh Models

Zicheng Zhang, Wei Sun, Tao Wang, Wei Lu, Xionghuo Min and Guangtao Zhai

Abstract—To improve the viewer’s Quality of Experience (QoE) and optimize computer graphics applications, 3D model quality assessment (3D-QA) has become an important task in the multimedia area. Point cloud and mesh are the two most widely used digital representation formats of 3D models, the visual quality of which is quite sensitive to lossy operations like simplification and compression. Therefore, many related studies such as point cloud quality assessment (PCQA) and mesh quality assessment (MQA) have been carried out to measure the caused visual quality degradations. However, a large part of previous studies utilizes full-reference (FR) metrics, which means they may fail to predict the quality level with the absence of the reference 3D model. Furthermore, few 3D-QA metrics are carried out to consider color information, which significantly restricts the effectiveness and scope of application. In this paper, we propose a no-reference (NR) quality assessment metric for colored 3D models represented by both point cloud and mesh. First, we project the 3D models from 3D space into quality-related geometry and color feature domains. Then, the natural scene statistics (NSS) and entropy are utilized to extract quality-aware features. Finally, the Support Vector Regressor (SVR) is employed to regress the quality-aware features into quality scores. Our method is mainly validated on the colored point cloud quality assessment database (SJTU-PCQA) and the colored mesh quality assessment database (CMDM). The experimental results show that the proposed method outperforms all the state-of-art NR 3D-QA metrics and obtains an acceptable gap with the state-of-art FR 3D-QA metrics. The code of the proposed model is publicly available now¹.

Index Terms—3D model quality assessment, colored point cloud, colored mesh, no-reference quality assessment, natural scene statistics

I. INTRODUCTION

Nowadays, with the rapid development of computer graphics, the digital representation of 3D models has been widely studied and used in a wide range of application scenarios such as virtual reality (VR), medical 3D reconstruction, and video post-production [1]. Among the common digital representation forms of 3D models, point cloud and mesh are the most widely used formats in practical. A point cloud based object is a set of points in space, in which each point is described with geometry coordinates and sometimes with other attributes such as color and surface normals. Mesh is more complicated because it is a collection of vertices, edges, and faces which together define the shape of a 3D model. Additionally, except for geometry information, the 3D mesh may also contain various appearance attributes, such as color and material. Both point cloud and mesh are able to vividly display exquisite models and complex scenes. However, since

point cloud and mesh record the omnidirectional details of objects and scenes, lossless 3D models usually need large storage space and very high transmission bandwidth in practical applications. Hence, diverse 3D processing algorithms are proposed to adapt to specific needs using processing operations such as simplification and compression, which inevitably cause damage to the visual quality of 3D models. Additionally, in some 3D scanning model APIs like Apple 3D object capture [2] and Intel Lidar Camera Realsense [3], some slight disturbance such as blur, noise, etc. may be introduced to the constructed 3D models.

Therefore, to improve users’ Quality of Experience (QoE) in 3D fields and optimize 3D compression and reconstruction systems, it is of great significance to develop quality metrics for point cloud quality assessment (PCQA) and mesh quality assessment (MQA). However, different from the format of 2D media like images and videos where pixels are distributed in the fixed grid, the points in 3D models are distributed irregularly in the space, which brings a huge challenge for 3D-QA tasks. For example, the neighborhood of pixels in 2D media can be easily obtained, thus the local features are available by analyzing the relationship between the pixel and its neighborhood. However, the neighborhood for points in 3D models is very ambiguous, which makes it difficult to construct local feature analysis. Furthermore, the geometrical shape of 2D media is fixed, which enables us to easily scale or crop the 2D media for feature extraction while similar operations are very hard to define for 3D models. Although many 3D-QA databases [4] [5] [6] [7] have been proposed to push forward the development of 3D-QA algorithms, the difficulty of collecting 3D models and conducting subjective experiments greatly limit the size of the 3D-QA databases, which may also restrict relevant research, especially for NR 3D-QA metrics.

A. Previous 3D-QA Works

Quality assessment can be divided into subjective quality assessment and objective quality assessment according to whether human observers are involved. It is known that, in subjective quality assessment, large numbers of people have to assess the visual quality of 3D models and give their subjective scores. Although the mean opinion scores (MOSs) collected from human observers are straightforward and precise, they cannot be used in practical applications due to the huge time consumption and high expense [8]. Therefore, objective quality metrics are urgently needed to predict the quality level of 3D models automatically. The objective quality

¹Manuscript updated July 30, 2021.

¹The code is available at <https://github.com/zzc-1998/NR-3DQA>.

assessment can then be divided into FR 3D-QA methods and NR 3D-QA methods. FR 3D-QA methods function by comparing the difference between the reference 3D models and distorted 3D models while NR 3D-QA methods only analyze the distorted 3D models to give the quality values. Considering the complexity of 3D models, in the literature, a large part of 3D-QA metrics are full-reference and only take geometry features into consideration [9]–[16]. When it comes to 3D models with color information, limited numbers of works have been proposed [17]–[20]. Clearly, the NR 3D-QA for colored models has fallen behind. In this section, we briefly review the development of 3D-QA and introduce the mainstream methods designed for 3D-QA tasks.

1) *The Development of PCQA*: FR-PCQA metrics operate by comparing the difference between the reference and distorted point clouds and they usually focus on the geometry aspect at the point level, such as p2point [9], p2plane [10], and p2mesh [13]. The p2point estimates the levels of distortion by computing the distance vector between the corresponding points. The p2plane further projects the distance vector on the normal orientation for evaluating the quality loss. The p2mesh first reconstructs the point cloud to mesh and then measures the distance from point to the reconstructed surface to predict the quality level, which greatly depends on the reconstruction algorithms and lacks stability. Since the point-level difference is difficult to reflect the complex structural distortions, some studies further consider other structural characteristics for PCQA. For example, Alexiou *et al.* [14] adopt the angular difference of point normals to estimate the degradations. Javaheri *et al.* [15] utilize the generalized Hausdorff distance to reflect the distortions caused by compression operations.

In some situations, color information can not be ignored, which challenges the geometry-based PCQA methods. To incorporate the color information into PCQA models, Meynet *et al.* [20] propose a metric (PCQM) to use the weighted linear combination of curvature and color information to evaluate the visual quality of distorted point cloud. Inspired by SSIM [21], Alexiou *et al.* [17] compute the similarity on four types of features, including geometry, normal vectors, curvature and color information. What’s more, some studies [4] [7] try to predict the quality level by evaluating the projected 2D images from 3D models. The advantage is that image quality assessment (IQA) metrics have been well developed while the disadvantage is that there is inevitable information loss during the projection and the projected images are easily affected by the projected angles and viewpoints.

To the best of our knowledge, there is only one NR-PCQA metric so far, which is a learning-based approach proposed in [22]. The author constructs a large-scale colored PCQA database and designs two modified PointNet [?] as feature extraction backbone for both geometrical and color attributes. However, the code and database have not been publicly available yet.

2) *The Development of MQA*: The MQA metrics can be categorized into two types: model-based metrics [11] [12] [16] [23] [24] which operate directly on the 3D models, and image quality assessment (IQA) based metrics [18] [19] [25] [26] [27] which operate on the rendering snapshots of 3D models.

Supported by the vast amount of previous research on FR IQA methods [28]–[30], many FR-MQA models have been proposed using similar manners, which usually compute local features at the vertex level and then pool the features into a quality value. For example, MSDM2 [11] uses the differences of structure (captured via curvature statistics) computed on local corresponding neighborhoods from the meshes being compared to predict the quality level. DAME [16] measures the differences in dihedral angles between the reference and the distorted meshes to evaluate the quality loss. FMPD [12] estimates the local roughness difference derived from Gaussian curvature to assess the quality of the distorted mesh. However, these metrics only take geometry information into consideration.

Furthermore, to analyze the influence of color information, some FR color-involved MQA metrics have been carried out. Tian *et al.* [18] introduce a global distance over texture image using Mean Squared Error (MSE) to quantify the effect of color information. Guo *et al.* [19] exploit SSIM to calculate the texture image distance as the color information features. Nehmé *et al.* [5] introduce a metric (CMDM) to incorporate perceptually-relevant curvature-based and color-based features to evaluate the visual quality of colored meshes.

Recently, thanks to the effectiveness of machine learning, some NR-MQA metrics based on machine learning have been proposed. Abouelaziz *et al.* [23] extract features using dihedral angle models and train a support vector machine for feature regression. Later, Abouelaziz *et al.* [24] scale the curvature and dihedral angle into 2D patches and utilize convolution neural network (CNN) for training. They [25] further introduce a CNN framework with saliency views rendered from 3D meshes. However, the NR methods mentioned above only extract geometry features and may fail to accurately predict the scores of colored meshes.

B. Our Approach

Generally speaking, a large part of the metrics mentioned above are full-reference, which can make full use of the relationship between the reference and distorted 3D models and give relatively accurate results. However, the disadvantage of FR 3D-QA metrics is also obvious, they are not able to work in the absence of reference 3D models. What’s more, in many application scenarios like 3D reconstruction, pristine reference is not always available. Therefore, inspired by the huge success of natural scene statistics (NSS) in IQA tasks [31] [32], we further utilize NSS to model quality-aware features for 3D models. Specifically, NSS is a discipline within the field of perception, which is dependent on the premise that the perceptual system is designed to interpret natural scenes [33]. NSS-based methods usually estimate the statistical parameters of feature distributions to quantify the distortion of natural scenes, which indicates that such methods are not sensitive to the shape and distributing pattern of data. Therefore, we propose an NR metric to predict the visual quality levels of colored 3D models based on natural scene statistics (NSS).

We first project the 3D models into corresponding quality-related geometry and color feature domains. Then, the natural

scene statistics (NSS) and entropy are utilized to extract these color and geometry characteristics. Finally, the obtained features are integrated into a quality value through the support vector regression (SVR) model. In order to test the effectiveness of different types of features and different kinds of distribution models, we test the performance of different combinations of the statistical parameters to find the optimal combination. Further, we conduct the computational efficiency experiment for comparison. The experimental results show that our method outperforms the mainstream NR metrics for 3D-QA and obtains an acceptable gap with the state-of-art FR 3D-QA metrics.

C. Contributions

We summarize our contributions as follows:

- To the best of our knowledge, we first introduce the NSS method, which has been widely adopted in many image quality assessment (IQA) studies, to 3D-QA fields. The NSS method can effectively break the restriction of the distributing pattern of 3D models and still obtain good performance.
- We conduct a no-reference quality assessment metric for both colored point cloud and mesh. We extract features not only from the geometry aspect, but also from the color aspect. Furthermore, it is the first method that can deal with both NR-PCQA and NR-MQA with color information. Our feature extraction and regression framework are very standard, which means it is easy to modify our metric for performance improvement or specific needs.
- We further investigate the effectiveness of different types of features (color and geometry) and different kinds of distribution models, which can provide useful guidelines for future research.
- Compared with the state-of-art methods, our method is more efficient in the computation process, which means the proposed method is potentially more capable of handling practical situations. The code of the proposed model is also released for promoting the development of NR 3D-QA.

The paper is organized as follows: Section II describes the feature projection processes. Section III describes the process of quantifying the distortions to statistical parameters. Section IV presents the experiment setup along with the experimental results. Section V summaries the content of this paper.

II. FEATURE PROJECTION

Given a distorted 3D object O , we define that:

$$O \in \{P, M\}, \quad (1)$$

$$P = \{Points\}, \quad (2)$$

$$M = \{Vertices, Edges, Faces\}, \quad (3)$$

where P and M mean that the 3D object is represented by point cloud and mesh respectively, and the color information is attached to *Points* in point cloud and *Vertices* in mesh respectively.

A. Geometry Feature Projection

Geometry features usually have a strong correlation with human perception, which has been firmly proved in 3D-QA studies [9]–[16]. Although the geometry features are computed in different ways for point cloud and mesh, they share similar characteristics for the visual quality of 3D models. In this section, we project the given 3D model into several quality-aware geometry feature domains:

$$F_{geo} = \mathbf{Projection}_{geo}(O), \quad (4)$$

$$O \in \{P, M\}, \quad (5)$$

where F_{geo} indicates the set of geometry feature domains of the 3D model, $\mathbf{Projection}_{geo}(\cdot)$ denotes the geometry projection function.

B. Point Cloud Geometry Feature Domains

Considering that the point cloud lacks surfaces, we first need to get the neighborhood set for each point so we can further extract the geometry features. Given the point cloud $P = \{p_i\}_{i=1}^N$, the neighborhood P_{Nbi} of each vertex p_i can be obtained utilizing the k -nearest neighbors (k -NN) algorithm:

$$P_{Nb} = \mathbf{KNN}_{k=10}(P), \quad (6)$$

$$Dist(p, q) = \sqrt{(p_x - q_x)^2 + (p_y - q_y)^2 + (p_z - q_z)^2}, \quad (7)$$

where N indicates the number of points in the point cloud, P_{Nb} is the set of all neighborhoods, $\mathbf{KNN}(\cdot)$ denotes the k -NN algorithm function, the k level is set as 10, and Euclidean distance is exploited as the distance function. With the computed neighborhood P_{Nbi} , the corresponding covariance matrix C_i for each point p_i can be denoted as:

$$C_i = \begin{bmatrix} \hat{p}_1 - \bar{p} \\ \dots \\ p_{\hat{K}_i} - \bar{p} \end{bmatrix}^T \cdot \begin{bmatrix} \hat{p}_1 - \bar{p} \\ \dots \\ p_{\hat{K}_i} - \bar{p} \end{bmatrix}, \hat{p}_1, \dots, p_{\hat{K}_i} \in Nb_i \quad (8)$$

where \hat{K}_i stands for the size of neighborhood P_{Nbi} , and \bar{p} represents the centroid of points in neighborhood Nb_i . Therefore, the eigenvector problem for the covariance matrix C_i can be described as below:

$$C_i \cdot v_j = \lambda_j \cdot v_j, j \in \{1, 2, 3\} \quad (9)$$

where $(\lambda_1, \lambda_2, \lambda_3)$ indicate the eigenvalues, (v_1, v_2, v_3) represent the corresponding eigenvectors, and we assume that $\lambda_1 > \lambda_2 > \lambda_3$. Thus, a total of 3 eigenvalues are obtained for each point p_i in the point cloud P .

In previous studies [34] [35], the eigenvalues mentioned above are used to calculate various geometry features for tasks like classification, simplification, and segmentation, which show great ability to describe the complicated geometry information and achieve outstanding performance in such tasks. Hence, we selected several geometry features that may be effective for point cloud quality assessment:

- **Curvature:** Curvature is the amount by which a curve deviates from being a straight line, which is frequently used to describe roughness or smoothness.
- **Anisotropy:** Anisotropy is used to exhibit variations in geometrical properties for different directions.

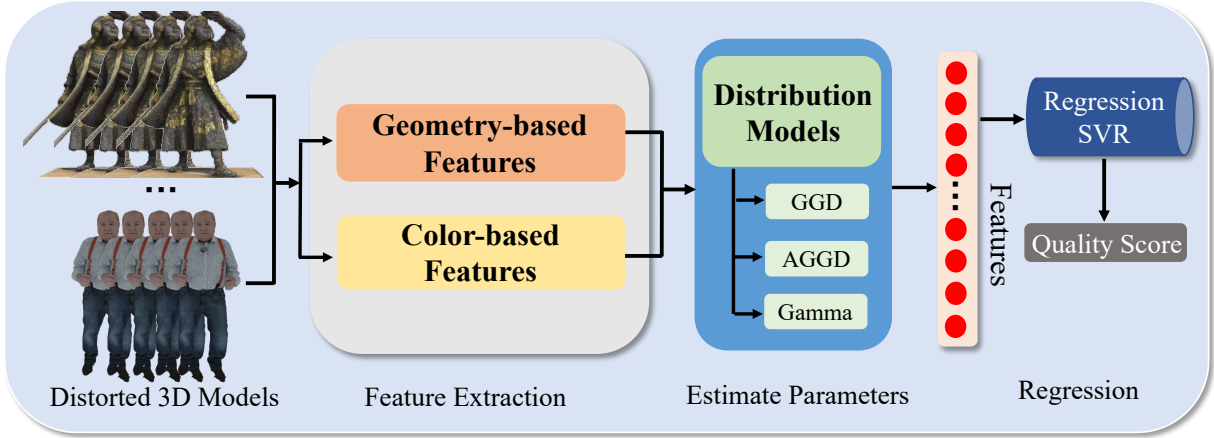


Fig. 1. Framework of the proposed method. Geometry-based and color-based features are first extracted from the distorted 3D models. Then various statistical parameters are estimated from the extracted features to form the feature vector. Finally, the quality scores are given through the SVR regression module.

- **Linearity:** Linearity is the property for estimating the similarity to a straight line.
- **Planarity:** Planarity is utilized to measure the similarity to a planar surface.
- **Sphericity:** Sphericity is the measure of how closely the shape of an object resembles that of a perfect sphere.

Additionally, all the geometry features described above are calculated at the point level, which indicates that each p_i has its own curvature, anisotropy, linearity, planarity, and sphericity. The formulations for geometry features are denoted as:

$$Cur(p_i) = \frac{\lambda_3}{\lambda_1 + \lambda_2 + \lambda_3}, \quad (10)$$

$$Ani(p_i) = \frac{\lambda_1 - \lambda_3}{\lambda_1}, \quad (11)$$

$$Lin(p_i) = \frac{\lambda_1 - \lambda_2}{\lambda_1}, \quad (12)$$

$$Pla(p_i) = \frac{\lambda_2 - \lambda_3}{\lambda_1}, \quad (13)$$

$$Sph(p_i) = \frac{\lambda_3}{\lambda_1}, \quad (14)$$

where $\lambda_1, \lambda_2,$ and λ_3 refer to the corresponding eigenvalues respectively. Through the operations mentioned above, the point cloud is transformed into 5 geometry feature domains.

C. Mesh Geometry Feature Domains

Among the common digital representation forms of 3D models, the 3D mesh is more complicated because it is a collection of vertices, edges, and faces which together define the shape of a 3D model. Therefore, the feature extraction process is different from that in the point cloud.

1) *Curvature:* Thanks to the edges and faces information contained in mesh, the computation of curvature is more precise than the point cloud. So far, various curvature definitions have been introduced for 3D meshes [36] [37], among which the average curvature is proven to be able to stably describe the local structural information of 3D meshes. Hence, a weighted average curvature method introduced in [37] is adopted to measure the roughness of embedded surfaces in

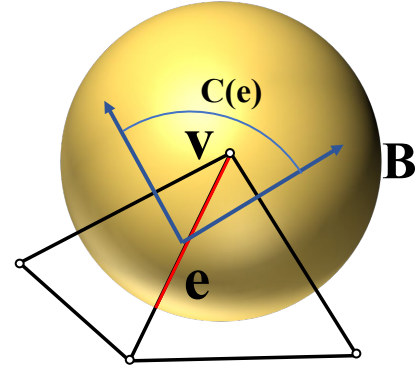


Fig. 2. Example of the variables corresponding to the curvature calculation, where the red line indicates $|e \cap B|$ and $C(e)$ indicates the curvature contribution of e .

3D meshes. Given the mesh $M = \{V, E, F\}$, the weighted average curvature is calculated by averaging the curvature contributions over a certain region B around each vertex v_i :

$$Cur(v_i) = \frac{1}{|B|} \sum_{e \in E} C(e) |e \cap B| \cdot \bar{e} e^t, \quad (15)$$

where $Cur(v_i)$ represents the weighted average curvature for vertex v , region B is a sphere region centered at v and its radius is 1/100 of the bounding box of the 3D mesh, $|B|$ stands for the surface area of region B . E is the set of edges that are linked to the vertex v , $C(e)$ indicates the curvature contribution of e (the signed angle between the normals of the two oriented triangles incident to edge e), $|e \cap B|$ denotes the weight which is defined as the length of $e \cap B$ (always between 0 and $|e|$) and \bar{e} is a unit vector in the same direction as e . An example of the variables corresponding to the curvature calculation is shown in Fig. 2.

2) *Dihedral Angle:* Normally speaking, dihedral angle is the angle between two planes. For a 3D mesh, the dihedral angle is the angle between the normals of two adjacent faces, which has been utilized in [38] as an effective indicator for measuring the loss of the mesh simplification. Furthermore, [16] exploits oriented dihedral angles instead of the simple

dot product of normals to better distinguish the convex and concave angles, which achieves great performance. Encouraged by similar ideas, we adopt the dihedral angles set to describe the visual quality of 3D meshes. Assuming that the vertices for two adjacent faces f_1 and f_2 are $\{v_1, v_3, v_4\}$ and $\{v_2, v_3, v_4\}$, we have:

$$Dih_{f_1, f_2} = \arccos(n_1 \cdot n_2) * \text{sgn}(n_1 \cdot (v_2 - v_1)), \quad (16)$$

where D_{f_1, f_2} is the oriented dihedral angle between two adjacent faces f_1 and f_2 , n_1 and n_2 are the normals of f_1 and f_2 , sgn denotes the signum function which is used to decide the orientation of the dihedral angle.

3) *Face Area and Angle*: Area and angle are two simple attributes of 3D mesh faces, which can be easily computed by making use of the coordinates of the face's vertices. In the mesh smoothing algorithm proposed in [39], attributes including face angle are used to predict the new location of the smoothed nodes. While in the 3D mesh encoding method introduced in [40], face angle is utilized to instruct the compression of 3D meshes, which indicates that face angle is related to the quality of 3D meshes. Therefore, to further measure the visual quality degradation of 3D meshes, the face area and angle are collected as feature sets.

Finally, the mesh is projected into 4 geometry feature domains:

- *Curvature*: The weighted average curvature is used to describe the geometry characteristics like roughness or smoothness.
- *Dihedral Angle*: Dihedral angle is employed as a useful descriptor for measuring the caused degradations.
- *Face Area & Angle*: These two attributes are highly correlated with the effectiveness of lossy operations like compression.

D. Color Feature Projection

Color is a significant aspect of visual quality assessment. The color information in the 3D models is usually stored in the form of RGB channels. However, the RGB color space has been proven to have a poor correlation with human perception. Additionally, the color presentation is different between point cloud and mesh. For a colored point cloud, the color is directly determined by the color information of the point, while for a colored mesh, the color of the surface is generally rendered by the color information of the contained vertices.

To better analyze the influence of color information, we convert the color information from RGB channels to LAB channels, which has been adopted in many quality assessment tasks [5] as the color projection for 3D models:

$$F_{color} = \mathbf{Projection}_{geo}(O), \quad (17)$$

$$O \in \{P, M\}, \quad (18)$$

where F_{color} indicates the set of color feature domains of the 3D model, $\mathbf{Projection}_{geo}(\cdot)$ stands for the color projection function, and P and M represent the distorted point cloud

and mesh respectively. And the detailed color transformation is formulated as below:

$$\begin{bmatrix} X \\ Y \\ Z \end{bmatrix} = \begin{bmatrix} 2.7688 & 1.7517 & 1.1301 \\ 1.0000 & 4.5906 & 0.0601 \\ 0 & 0.0565 & 5.5942 \end{bmatrix} \begin{bmatrix} R \\ G \\ B \end{bmatrix}, \quad (19)$$

$$\begin{cases} L = 116f\left(\frac{Y}{Y_n}\right) - 16, \\ A = 500\left(f\left(\frac{X}{X_n}\right) - f\left(\frac{Y}{Y_n}\right)\right), \\ B = 200\left(f\left(\frac{Y}{Y_n}\right) - f\left(\frac{Z}{Z_n}\right)\right), \end{cases} \quad (20)$$

where R, G, B represent the corresponding RGB color channels, X, Y, Z stand for the corresponding XYZ color channels, L, A, B denote the corresponding RGB color channels, and X_n, Y_n, Z_n describe specified white achromatic reference illuminant. The $f(\cdot)$ function is described as:

$$f(t) = \begin{cases} \sqrt[3]{t}, & \text{if } t > \delta^3, \\ \frac{t}{3\delta^2} + \frac{4}{29}, & \text{otherwise,} \end{cases} \quad (21)$$

where δ is set as $\frac{6}{29}$. Finally, the LAB color channels are computed as the color feature domains.

III. ESTIMATING STATISTICAL PARAMETERS

Through prior knowledge and observations of the corresponding feature distributions, we choose entropy and several NSS models including the generalized Gaussian distribution (GGD), the general asymmetric generalized Gaussian distribution (AGGD), and the shape-rate Gamma distribution for parameters estimation.

A. Basic Statistical Parameters

With the set of various features, we exploit the normalization operation as the pre-processing:

$$\hat{F} = \frac{F - \text{mean}(F)}{\text{std}(F) + C}, \quad (22)$$

$$F \in \{F_{geo}, F_{color}\}, \quad (23)$$

where F represents the feature domain, $\text{mean}(\cdot)$ is the average function, $\text{std}(\cdot)$ denotes the standard deviation function, C is a small constant to avoid instability and F_{geo} and F_{color} indicate the geometry and color feature domains respectively. The average and standard deviation values of each feature domain are also collected. Fig. 4 presents the LAB normalized probability distributions of the color quantization distortion. It can be observed that with the increasing quantization levels, the corresponding distributions become significantly sparse. Considering that some simplification and compression algorithms usually introduce such quantization operations to the 3D models which cause the distribution of geometry features also has similar phenomena. Hence, we propose to use entropy to measure the information loss:

$$E = \mathbf{Entropy}(F), \quad (24)$$

$$F \in \{F_{geo}, F_{color}\}, \quad (25)$$

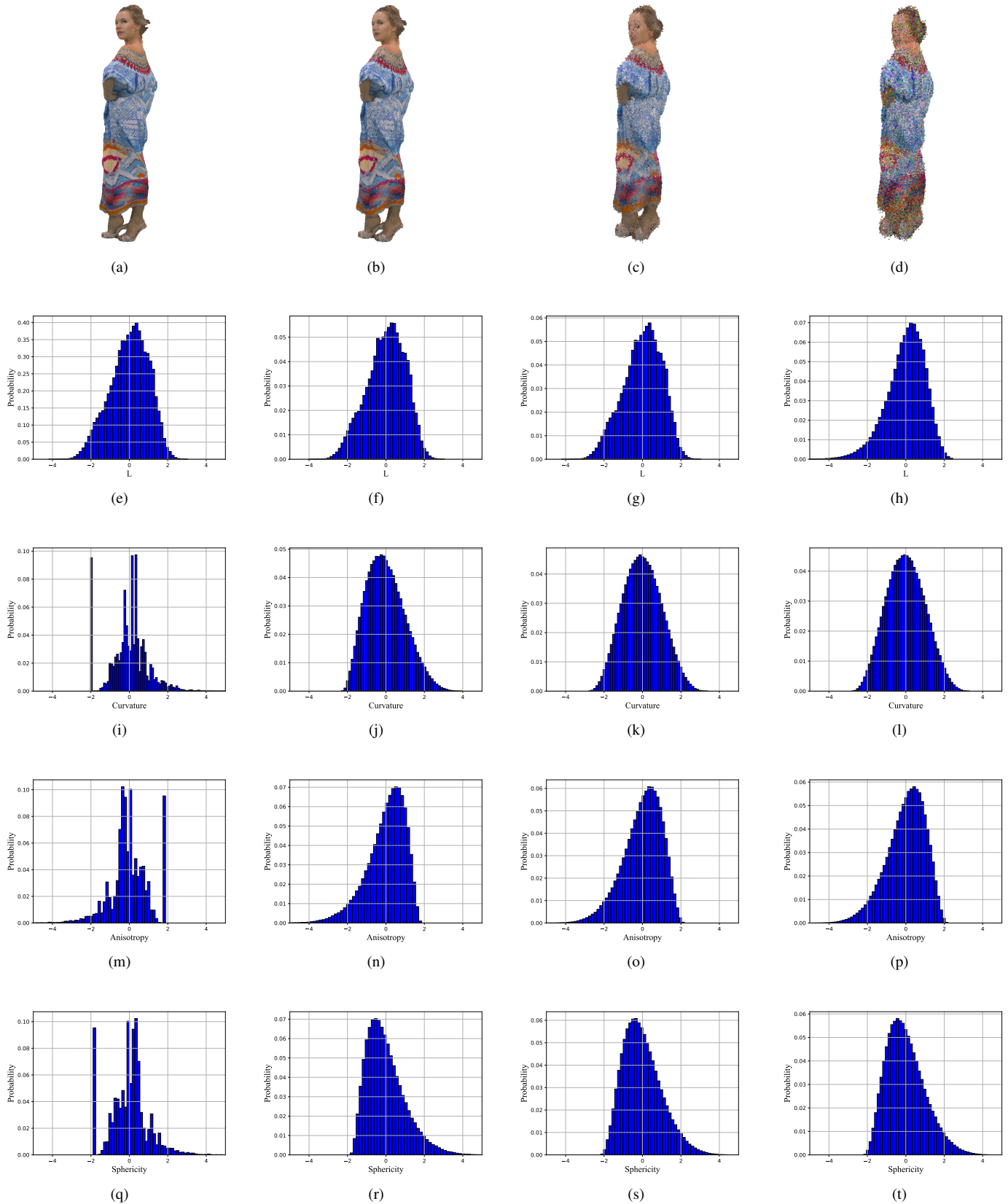


Fig. 3. Examples of point cloud samples from SJTU-PCQA database [4]. (a), (b), (c), and (d) are 4 distorted point cloud samples with increasing distortion levels. Some features' (L , Cur , Ani , Sph) normalized probability distributions are selected as examples. More specifically, (e), (i), (m), and (q) are the corresponding features' normalized probability distributions of (a) model, (f), (j), (n), and (r) are the corresponding features' normalized probability distributions of (b) model, (g), (k), (o), and (s) are the corresponding features' normalized probability distributions of (c) model, (h), (l), (p), and (t) are the corresponding features' normalized probability distributions of (d) model respectively.

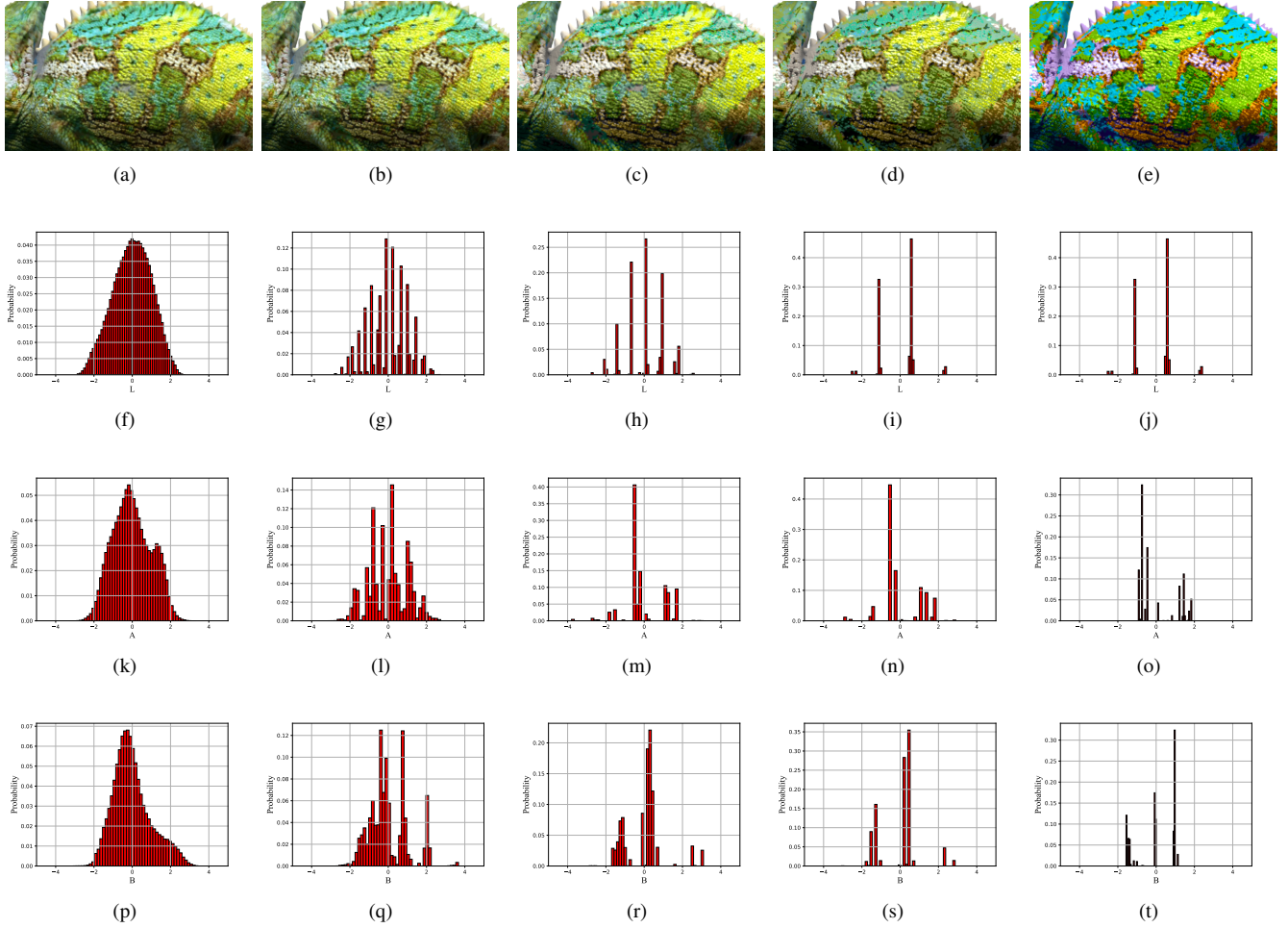


Fig. 4. A comparison example for color distortion in the CMDM database [5]. (a) represents the snapshots of the reference 3D mesh while (b)-(e) stands for the snapshots of the meshes with 4 increasing levels of color information quantization. (f), (k), (p) represent the LAB normalized probability distributions for (a) model, (g), (l), (q) represent the LAB normalized probability distributions for (b) model, (h), (m), (r) represent the LAB normalized probability distributions for (c) model, (i), (n), (s) represent the LAB normalized probability distributions for (d) model, and (j), (o), (t) represented the LAB normalized probability distributions for (e) model respectively.

B. GGD Parameters

Fig. 3 shows 4 distorted point cloud samples with increasing distortion levels and their corresponding geometry features' normalized probability distributions. It can be observed that some of the feature distributions tend to be Gaussian-like, especially for the geometry distributions after distorted operations. Obviously, with higher levels of distortions, the shape and scale of the distributions vary from each other. To capture the characteristics of 3D model distributions at the general level, we propose to use the generalized Gaussian distribution (GGD):

$$GGD(x; \alpha, \beta^2) = \frac{\alpha}{2\beta\Gamma(1/\alpha)} \exp\left(-\left(\frac{|x|}{\beta}\right)^\alpha\right), \quad (26)$$

$$x \in \{F_{geo}, F_{color}\},$$

where $\beta = \sigma\sqrt{\frac{\Gamma(1/\alpha)}{\Gamma(3/\alpha)}}$, $\Gamma(\alpha) = \int_0^\infty t^{\alpha-1}e^{-t}dt$, $\alpha > 0$ is the gamma function, and the two estimated parameters (α, β^2) indicate the shape and variance of the distribution. What's more, considering that the variance for normalized

distribution is fixed as 1, we estimate the GGD parameters from distributions before normalization.

C. AGGD Parameters

However, in some situations, the shape of the distribution is not symmetrical. We can see clearly from Fig. 3 that the anisotropy distributions for the (b)-(d) models have longer tails on the left while the sphericity distributions for the (b)-(d) models have longer tails on the right. Inspired by [31], we utilize the general asymmetric generalized Gaussian distribution (AGGD) model to extract more detailed parameters from normalized feature distributions to describe the different spread extent in two directions:

$$AGGD(x; v, \sigma_l^2, \sigma_r^2) = \begin{cases} \frac{v}{(\beta_l + \beta_r)\Gamma(\frac{1}{v})} \exp\left(-\left(\frac{-x}{\beta_l}\right)^v\right) & x < 0, \\ \frac{v}{(\beta_l + \beta_r)\Gamma(\frac{1}{v})} \exp\left(-\left(\frac{x}{\beta_r}\right)^v\right) & x \geq 0, \end{cases} \\ x \in \{F_{geo}, F_{color}\}, \quad (27)$$

where $\beta_l = \sigma_l \sqrt{\frac{\Gamma(\frac{1}{v})}{\Gamma(\frac{3}{v})}}$, $\beta_r = \sigma_r \sqrt{\frac{\Gamma(\frac{1}{v})}{\Gamma(\frac{3}{v})}}$, $\eta = (\beta_r - \beta_l)$, the parameter v decides the shape of the distribution, σ_l^2 and σ_r^2 are scale parameters that refer to the spread extent on the left and right side of the distribution respectively, η is a parameter that can better fit the AGGD model stated in [31]. Additionally, the AGGD can be recognized as the extension of GGD. Furthermore, when $\sigma_l^2 = \sigma_r^2$, the AGGD turns into GGD. The four parameters ($\eta, v, \sigma_l^2, \sigma_r^2$) are able to obtain more representative characteristics of asymmetric distribution.

D. Gamma Parameters

In previous 3D-QA studies [41], Gamma distribution is usually employed as the estimated distribution and has been proven effective. Hence, we also adopt Gamma distribution to estimate statistical parameters. The shape-rate Gamma model is formulated as:

$$\text{Gamma}(x; \alpha, \beta) = \frac{\beta^\alpha x^{\alpha-1} e^{-\beta x}}{\Gamma(\alpha)} x > 0, \quad (28)$$

$$x \in \{\hat{F}_{geo}, \hat{F}_{color}\},$$

where α and β stands for the shape and rate parameters and $\alpha, \beta > 0$.

In summary, we collect the average, standard deviation, and entropy values as the fundamental features. Then we use 3 representative distribution models to estimate 8 statistical parameters, including GGD (α, β^2), AGGD ($\eta, v, \sigma_l^2, \sigma_r^2$), Gamma (α, β), for all feature domains. Finally, considering that the colored point cloud has 8 feature domains (*Cur, Ani, Lin, Pla, Sph, L, A, B*) and the colored mesh has 7 feature domains (*Cur, Dhi, Far, Fan, L, A, B*), 88 (8×11) features are computed for a single colored point cloud and 77 (7×11) features are computed for a single colored mesh respectively. The summary of features extracted in the proposed method is listed in Table I.

E. Regression Model

After the feature extraction process, a feature vector is obtained to describe the characteristics of the 3D model. In our experiment, we propose to use the support vector machine regressor (SVR) as the regression model, which is a common and effective choice to handle high dimensional data in previous quality assessment research [23] [31]. Then the feature vector can be integrated into a quality score for evaluation. We employ the Python sklearn package [42] to implement the radial basis function (RBF) kernel SVR model with default settings.

IV. EXPERIMENT EVALUATION

A. Experiment Setup

1) *Experiment Setup for PCQA*: The large-scale point cloud quality assessment database constructed in [22] has not been public yet. Therefore, to test the performance of the proposed method, we utilize the subjective point cloud assessment (SJTU-PCQA) database introduced in [4]. The SJTU-PCQA database provides 420 point cloud samples distorted from

10 reference point clouds. Each reference point cloud is distorted with seven types of common distortions, including compression noise, color noise, Gaussian geometric shift, downsampling loss, etc. Each kind of distortion is adjusted with six levels, which generates 42 (7×6) distorted point cloud samples for every reference point cloud. Unfortunately, only 9 reference point clouds and their corresponding distorted point cloud samples are now available in the public, thus we can obtain 378 (9×42) point cloud samples for the experiment.

Since the proposed approach requires a training procedure to calibrate the SVR model and to avoid the influence of similar contents, we select 7 of the 9 groups of point clouds as training set and leave the rest 2 groups as testing set. In order to ensure the validity of the results, we exhaustively list all the $C_9^7=36$ database separations for the experiment and use the average performance as the final experimental results.

Considering that limited numbers of NR-PCQA metrics for colored point clouds have been proposed (the learning-based no-reference approach in [22] has not open source yet), we select mostly full-reference metrics for comparison. The comparison QA metrics can be categorized into two types:

- *Image-based metrics*: These metrics evaluate the quality of 3D models by assessing the quality of the corresponding 2D projections. Please refer to [4] for detailed projection process. The FR image-based metrics include PSNR, SSIM [21], MS-SSIM [28], IW-SSIM [43], FSIM [29], VIF [30], and PB-PCQA [4]. The NR image-based metrics include NIQE [44] and BRISQUE [31].
- *Model-based metrics*: These metrics operate directly from the 3D model and are all full-reference, which include p2point [9], p2plane [10], and PCQM [20].

To further test the effectiveness and contributions of different types of features (color and geometry) and different statistical parameters, we split the features into 8 groups: (1) P1: mean, standard deviation, and entropy values of geometry feature domains; (2) P2: GGD parameters of geometry feature domains; (3) P3: AGGD parameters of geometry feature domains; (4) P4: Gamma distribution parameters of geometry feature domains; (5) P5: mean, standard deviation, and entropy values of color feature domains; (6) P6: GGD parameters of color feature domains; (7) P7: AGGD parameters of color feature domains; (8) P8: Gamma distribution parameters of color feature domains. Then we can analyze the features' contributions by obtaining the performance of different combinations of feature groups. For example, the P2+P6 model only contains AGGD parameters of both geometry and color feature domains while the P1-P4 model only consists of statistical parameters of geometry feature domains.

2) *Experiment Setup for MQA*: The MQA method proposed in this paper is validated on the color mesh distortion measure (CMDM) database [5]. The database is generated from 5 source models subjected to geometry and color distortions. Then the source models are corrupted with 4 types of distortions based on color and geometry and each type of distortion is adjusted with 4 different strengths. The selected distortions are able to represent the common visual quality loss, which can usually be perceived during typical 3D model processing. There are 80 distorted models in this database and each

TABLE I
SUMMARY OF FEATURES EXTRACTED IN THE PROPOSED METHOD

Format	Feature Domains	Feature ID	Feature Description	Computation
Point cloud	$(Cur, Ani, Lin, Pla, Sph, L, A, B)$	$f_{p1} - f_{p16}$	Mean and standard deviation for each feature domain	Eq.(22)
	$(Cur, Ani, Lin, Pla, Sph, L, A, B)$	$f_{p17} - f_{p24}$	Entropy for each feature domain	Eq.(24)
	$(Cur, Ani, Lin, Pla, Sph, L, A, B)$	$f_{p25} - f_{p40}$	GGD (α, β^2) for each feature domain	Eq.(26)
	$(Cur, Ani, Lin, Pla, Sph, L, A, B)$	$f_{p41} - f_{p72}$	AGGD $(\eta, v, \sigma_l^2, \sigma_l^2)$ for each normalized feature domain	Eq.(27)
	$(Cur, Ani, Lin, Pla, Sph, L, A, B)$	$f_{p73} - f_{p88}$	Gamma (α, β) for each normalized feature domain	Eq.(28)
Mesh	$(Cur, Dhi, Far, Fan, L, A, B)$	$f_{m1} - f_{m14}$	Mean and standard deviation for each feature domain	Eq.(22)
	$(Cur, Dhi, Far, Fan, L, A, B)$	$f_{m15} - f_{m21}$	Entropy for each feature domain	Eq.(24)
	$(Cur, Dhi, Far, Fan, L, A, B)$	$f_{m22} - f_{m35}$	GGD (α, β^2) for each feature domain	Eq.(26)
	$(Cur, Dhi, Far, Fan, L, A, B)$	$f_{m36} - f_{m63}$	AGGD $(\eta, v, \sigma_l^2, \sigma_l^2)$ for each normalized feature domain	Eq.(27)
	$(Cur, Dhi, Far, Fan, L, A, B)$	$f_{m64} - f_{m77}$	Gamma (α, β) for each normalized feature domain	Eq.(28)

TABLE II
PERFORMANCE COMPARISON WITH COMPETITORS ON THE SJTU-PCQA DATABASE WHERE THE METRICS MARKED WITH * ARE PROPOSED METHODS.

Ref	Type	Metric	PLCC	SRCC	RMSE
FR	Image-based	PSNR	0.2481	0.2512	2.3354
		SSIM	0.3654	0.2789	2.2440
		MS-SSIM	0.3659	0.2592	2.2437
		IW-SSIM	0.4339	0.3285	2.1720
		FSIM	0.3196	0.3019	2.2843
		VIF	0.5243	0.5647	2.0653
		PB-PCQA	0.6076	0.6020	1.8635
	Model-based	p2point	0.0466	0.7009	2.4081
		p2plane	0.0462	0.6881	2.4080
		PCQM	0.8603	0.8465	1.2291
NR	Image-based	NIQE	0.3262	-0.1149	2.2788
		BRISQUE	0.3167	0.3066	2.3428
	Model-based	(P1+P5)*	0.7522	0.7449	1.7004
		(P2+P6)*	0.7173	0.6973	1.7581
		(P3+P7)*	0.6106	0.6122	2.0208
		(P4+P8)*	0.5841	0.4999	2.0469
		(P1-P4)*	0.7314	0.7137	1.8096
		(P5-P8)*	0.2351	0.2408	2.4511
		All groups*	0.7294	0.6887	1.8059

distorted model is provided with 5 subjective scores according to its viewpoints and animation types. For simplification, we use the average of the 5 subjective scores as the final quality score for the distorted model.

Similarly in the literature, few metrics are proposed to deal with the 3D-QA tasks of color meshes. In order to evaluate the performance of the proposed method, some image-based metrics that might be able to predict the visual quality of 3D meshes are utilized as competitors. Unfortunately, few no-reference quality assessment metrics for 3D meshes are open-sourced, thus we try to reproduce some of the metrics. Specifically, the metrics used for comparison can be divided into two types:

- Image-based metrics: These metrics operate by evaluating

TABLE III
PERFORMANCE COMPARISON WITH COMPETITORS ON THE CMDM DATABASE WHERE THE METRICS MARKED WITH * ARE PROPOSED METHODS.

Ref	Type	Metric	PLCC	SRCC	KRCC	RMSE	
FR	Image-based	PSNR	0.7672	0.7735	0.7280	0.8832	
		SSIM	0.7944	0.7817	0.7000	0.9656	
		MS-SSIM	0.8112	0.8029	0.8167	1.0019	
		FSIM	0.7786	0.8264	0.7800	1.0245	
		VIF	0.7901	0.7882	0.7333	0.8800	
	Model-based	CMDM	0.9130	0.9000	-	-	
	NR	Image-based	NIQE	0.4059	0.4768	0.3000	1.3352
			BRISQUE	0.5786	0.4882	0.3598	1.2237
		Model-based	NR-SVR	0.6082	0.4489	0.3420	1.3147
			NR-GRNN	0.6599	0.6948	0.5130	1.1121
NR-CNN			0.5204	0.5022	0.3420	1.2804	
(M1+M5)*			0.8781	0.8530	0.6955	0.6019	
(M2+M6)*			0.7819	0.7392	0.5821	0.7646	
(M3+M7)*			0.8342	0.7974	0.6456	0.6989	
(M4+M8)*			0.5982	0.5262	0.3951	0.9956	
(M1-M4)*			0.6561	0.5076	0.3954	0.9267	
(M5-M8)*	0.2985	0.1820	0.2283	1.2469			
All groups*	0.8826	0.8754	0.7222	0.6062			

the quality of 2D images rendered from the 3D colored meshes. The FR image-based metrics include PSNR, SSIM [21], MS-SSIM [28], IW-SSIM [43], FSIM [29], and VIF [30]. The NR image-based metrics include NIQE [44] and BRISQUE [31].

- Model-based metrics: The FR-MQA metric include CMDM [5]. The NR-MQA metrics designed especially for 3D meshes usually without color include NR-SVR [23], NR-GRNN [45], NR-CNN [24].

For the same purpose to evaluate the effectiveness and contributions of different features, we categorize the features into 8 feature groups as well: (1) M1: mean, standard deviation, and entropy values of geometry feature domains; (2) M2: GGD parameters of geometry feature domains; (3) M3: GGD parameters of geometry feature domains; (4) M4: Gamma

distribution parameters of geometry feature domains; (5) M5: mean, standard deviation, and entropy values of color feature domains; (6) M6: GGD parameters of color feature domains; (7) M7: AGGD parameters of color feature domains; (8) M8: Gamma distribution parameters of color feature domains.

B. Experiment Criterion

Four mainstream consistency evaluation criteria are utilized to compare the correlation between the predicted scores and MOSs, which include Spearman Rank Correlation Coefficient (SRCC), Kendall’s Rank Correlation Coefficient (KRCC), Pearson Linear Correlation Coefficient (PLCC), and Root Mean Squared Error (RMSE). An excellent model should obtain values of SRCC, KRCC, and PLCC close to 1, and the value of RMSE near 0.

Specifically, to maintain the same experiment evaluation setup in [4], we select SRCC, PLCC, and RMSE as the judging criteria for the SJTU-PCQA database. For the CMDM database, we select all four criteria mentioned above.

C. Performance Discussion

In this section, we discuss the experimental performance, where our method achieves first place among all the NR methods on both the SJTU-PCQA database and the CMDM database.

1) *PCQA on the SJTU-PCQA Database*: The experimental results for PCQA on the SJTU-PCQA database are shown in Table II and the top 2 performance results in each column are marked in bold. We can see clearly that the FR-PCQA metric PCQM outperforms other PCQA metrics, which indicates that PCQM is effective at predicting the quality levels of colored point clouds. The P1+P5 model of our proposed method achieves second place among all FR and NR-PCQA metrics. Although the best performance of our method still has a gap with FR model PCQM, our method is more competitive than the widely used FR models such as p2point and p2plane. Considering that our method does not need original point clouds for reference, we can draw the conclusion that the proposed method does have a certain ability to extract quality-aware features and gives relatively accurate quality levels for colored point clouds. What’s more, since there are no related public NR QA models specifically designed for colored point cloud in literature, the proposed NR-PCQA model provides a competitive baseline for following NR-PCQA studies.

2) *MQA on the CMDM Database*: Table III presents the experimental results on the CMDM database and the top 2 performance results in each column are marked in bold. Surprisingly, the FR image-based metrics get remarkable performance results. However, such methods highly rely on the quality of the projected 2D images, which can be easily affected by projected angles and viewpoints. The NR model-based MQA methods such as NR-SVR, NR-GRNN, and NR-CNN have a stronger ability to predict the visual quality than the NR image-based MQA methods, but they do not take color information into consideration, thus resulting in lower performance than the proposed method. The FR-MQA metric CMDM achieves first place in PLCC and SRCC and the all

groups model in the proposed method obtains the second rank in PLCC and SRCC. Since CMDM is full-reference and the proposed method is no-reference, it can be concluded that the proposed method is also effective at predicting the quality score of colored meshes.

D. Statistical Test

To further analyze the performance of the proposed method, we conduct the statistical test in this section. We follow the same experiment setup as in [46] and compare the difference between the predicted quality scores with the subjective ratings. Specifically, we choose the P1+P5 model of the proposed PCQA metric and the all groups model of the proposed MQA metric for comparison. All possible pairs of models are tested and the results are listed in Fig. 5. It is obvious that our method is significantly superior to all compared NR metrics. We can also see that the FR metric PCQM achieves significantly better performance than our method, the FR metric CMDM is insignificantly distinguishable from our method.

E. Ablation Experiment

In this section, we analyze the results of the ablation experiment shown in Table II and Table III. The proposed P1-P4 model represents feature groups with only color features and the proposed P5-P8 model represents feature groups with only geometry features. It can be observed that the geometry features contribute more to the final quality score on the SJTU-PCQA database. By analyzing the different performance of different distribution models, we can see that the Gamma model achieves the poorest performance while the mean, standard deviation, and entropy values obtain the best performance, which indicates that the simpler statistical parameters can capture more representative characteristics on the SJTU-PCQA database.

The proposed M1-M4 model represents feature groups with only color features and the proposed M5-M8 model represents feature groups with only geometry features. Similarly, the geometry features make more contributions. However, unlike the situations on the PCQA database, the all groups model gets the highest performance in the proposed method, which indicates that all the statistical parameters are effective on the CMDM database.

F. Computational Efficiency

Considering that the proposed method operates directly from the 3D model, we also focus on computational efficiency. The image-based metrics usually operate quite fast due to the mature development of IQA metrics. Therefore, to make the comparison meaningful, we select the state-of-art FR method PCQM which achieves the best performance on the SJTU-PCQA database as the competitor. We conduct the test on a computer with Intel (R) Core (TM) i5-3470 CPU @ 3.20 GHz and 8 GB RAM. The time cost results are shown in Fig. 6, and we can see clearly that for the most point cloud models in the SJTU-PCQA database, the proposed method is more efficient than PCQM. The average time cost for the proposed

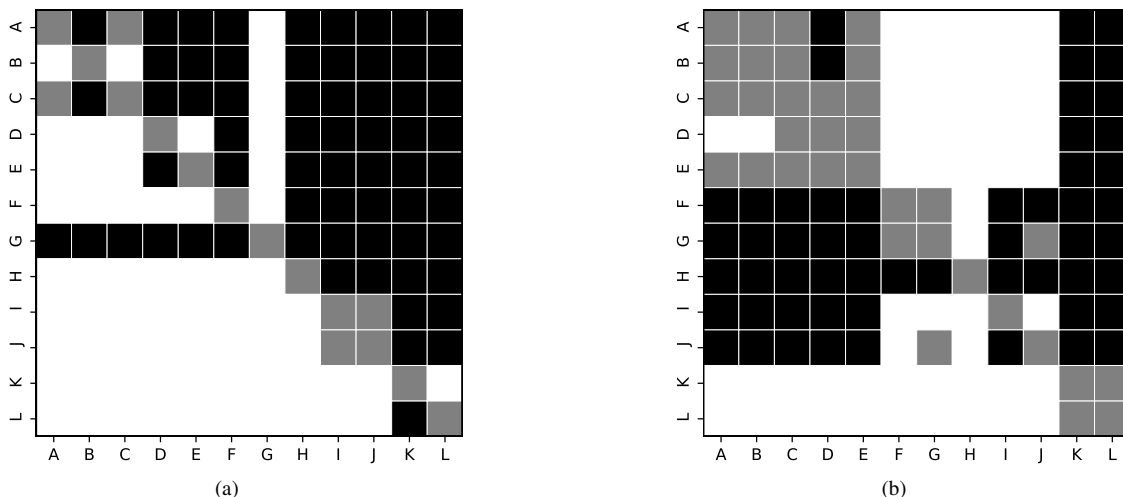


Fig. 5. Statistical test results of the proposed method and compared metrics on the SJTU-PCQA and CMDM databases. A black/white block means the row method is statistically worse/better than the column one. A gray block means the row method and the column method are statistically indistinguishable. The metrics denoted by A-L in (a) are of the same order as the compared metrics in Table II and M indicates the P1+P5 model of the proposed PCQA method, while the metrics denoted by A-K in (b) are of the same order as the compared metrics in Table III and L indicates the all groups model of the proposed MQA method respectively.

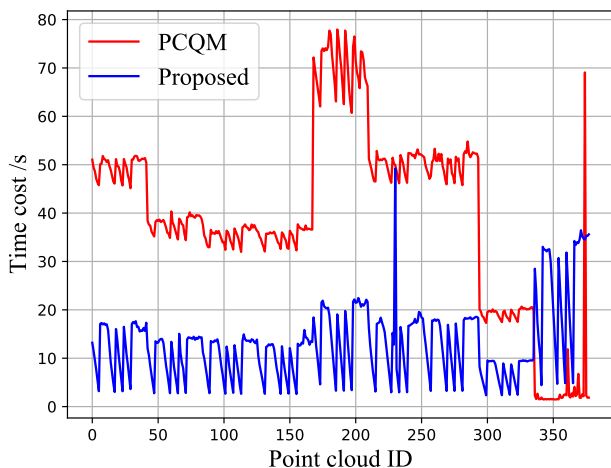


Fig. 6. Time cost comparison between PCQM and proposed method on the SJTU-PCQA database. Point cloud ID refers to the arrangement order of point clouds in the SJTU-PCQA database.

method is 13.02 seconds per point cloud while the average time cost for PCQM is about 39.14 seconds per point cloud. Although FR method PCQM needs to load both reference and distorted point cloud models at the same time and the proposed NR method only needs to load the distorted point cloud model, our method still costs a third of the time on average, which indicates that our method achieves relatively considerable computational efficiency.

V. CONCLUSION

This paper proposes a no-reference colored 3D model quality assessment metric based on entropy and natural scene statistics. The proposed method deals with the quality assessment problems for both mesh and point cloud. We first project the 3D models into corresponding quality-related geometry

and color feature domains. Then entropy and various NSS-based statistical parameters are estimated to better capture the representative characteristics and quantify the distortions that are more in line with human perception. The proposed method is validated on the colored point cloud quality assessment database (SJTU-PCQA) and the colored mesh quality assessment database (CMDM), both of which include geometry distortions and color distortions. The experimental results show that our method outperforms the mainstream NR 3D-QA metric competitors and obtains an acceptable gap with the state-of-art FR 3D-QA metrics. The quality assessment we propose is quite standard and can be easily modified and expanded to satisfy specific needs, which has great application potential. The code of the proposed model is also released for promoting the development of NR 3D-QA.

REFERENCES

- [1] H. Graf, S. P. Serna, and A. Stork, "Adaptive quality meshing for "on-the-fly" volumetric mesh manipulations within virtual environments," in *IEEE Symposium on Virtual Environments, Human-Computer Interfaces and Measurement Systems*, 2006, pp. 178–183.
- [2] "Apple developer document: Scanning and detecting 3d objects." [Online]. Available: https://developer.apple.com/documentation/arkit/content_anchors/scanning_and_detecting_3d_objects
- [3] "Intel realsense." [Online]. Available: <https://www.intelrealsense.com/>
- [4] Q. Yang, H. Chen, Z. Ma, Y. Xu, R. Tang, and J. Sun, "Predicting the perceptual quality of point cloud: A 3d-to-2d projection-based exploration," *IEEE Transactions on Multimedia*, pp. 1–1, 2020.
- [5] Y. Nehmé, F. Dupont, J. P. Farrugia, P. Le Callet, and G. Lavoué, "Visual quality of 3d meshes with diffuse colors in virtual reality: Subjective and objective evaluation," *IEEE Transactions on Visualization and Computer Graphics*, vol. 27, no. 3, pp. 2202–2219, 2021.
- [6] E. Alexiou, I. Viola, T. M. Borges, T. A. Fonseca, R. L. de Queiroz, and T. Ebrahimi, "A comprehensive study of the rate-distortion performance in mpeg point cloud compression," *APSIPA Transactions on Signal and Information Processing*, vol. 8, p. e27, 2019.
- [7] E. M. Torlig, E. Alexiou, T. A. Fonseca, R. L. de Queiroz, and T. Ebrahimi, "A novel methodology for quality assessment of voxelized point clouds," in *Applications of Digital Image Processing XLI*, vol. 10752. International Society for Optics and Photonics, 2018, pp. 174 – 190.

- [8] W. Sun, X. Min, G. Zhai, and S. Ma, "Blind quality assessment for in-the-wild images via hierarchical feature fusion and iterative mixed database training," 2021.
- [9] P. Cignoni, C. Rocchini, and R. Scopigno, "Metro: Measuring error on simplified surfaces," *Computer Graphics Forum*, vol. 17, no. 2, pp. 167–174, 1998.
- [10] R. Mekuria and P. Cesar, "Mp3dgc-pcc, open source software framework for implementation and evaluation of point cloud compression," 2016, p. 1222–1226.
- [11] G. Lavoué, "A multiscale metric for 3d mesh visual quality assessment," *Computer Graphics Forum*, vol. 30, no. 5, pp. 1427–1437, 2011.
- [12] K. Wang, F. Torkhani, and A. Montanvert, "A fast roughness-based approach to the assessment of 3d mesh visual quality," *Computers and Graphics*, vol. 36, no. 7, pp. 808–818, 2012.
- [13] D. Tian, H. Ochimizu, C. Feng, R. Cohen, and A. Vetro, "Geometric distortion metrics for point cloud compression," in *IEEE International Conference on Image Processing*, 2017, pp. 3460–3464.
- [14] E. Alexiou and T. Ebrahimi, "Point cloud quality assessment metric based on angular similarity," in *IEEE International Conference on Multimedia and Expo*, 2018, pp. 1–6.
- [15] A. Javaheri, C. Brites, F. Pereira, and J. Ascenso, "A generalized hausdorff distance based quality metric for point cloud geometry," in *International Conference on Quality of Multimedia Experience*, 2020, pp. 1–6.
- [16] L. Váša and J. Rus, "Dihedral angle mesh error: a fast perception correlated distortion measure for fixed connectivity triangle meshes," *Computer Graphics Forum*, vol. 31, no. 5, pp. 1715–1724, 2012.
- [17] E. Alexiou and T. Ebrahimi, "Towards a point cloud structural similarity metric," in *IEEE International Conference on Multimedia Expo Workshops*, 2020, pp. 1–6.
- [18] D. Tian and G. AlRegib, "Batex3: Bit allocation for progressive transmission of textured 3-d models," *IEEE Transactions on Circuits and Systems for Video Technology*, vol. 18, no. 1, pp. 23–35, 2008.
- [19] J. Guo, V. Vidal, I. Cheng, A. Basu, A. Baskurt, and G. Lavoué, "Subjective and objective visual quality assessment of textured 3d meshes," vol. 14, no. 2, 2016.
- [20] G. Meynet, Y. Nehmé, J. Digne, and G. Lavoué, "Pcqm: A full-reference quality metric for colored 3d point clouds," in *International Conference on Quality of Multimedia Experience*, 2020, pp. 1–6.
- [21] Z. Wang, A. Bovik, H. Sheikh, and E. Simoncelli, "Image quality assessment: from error visibility to structural similarity," *IEEE Transactions on Image Processing*, vol. 13, no. 4, pp. 600–612, 2004.
- [22] Y. Liu, Q. Yang, Y. Xu, and L. Yang, "Point cloud quality assessment: Large-scale dataset construction and learning-based no-reference approach," 2020.
- [23] I. Abouelaziz, M. El Hassouni, and H. Cherifi, "No-reference 3d mesh quality assessment based on dihedral angles model and support vector regression," in *Image and Signal Processing*, 2016, pp. 369–377.
- [24] I. Abouelaziz, M. E. Hassouni, and H. Cherifi, "A convolutional neural network framework for blind mesh visual quality assessment," in *IEEE International Conference on Image Processing*, 2017, pp. 755–759.
- [25] I. Abouelaziz, A. Chetouani, M. El Hassouni, L. J. Latecki, and H. Cherifi, "No-reference mesh visual quality assessment via ensemble of convolutional neural networks and compact multi-linear pooling," *Pattern Recognition*, vol. 100, p. 107174, 2020.
- [26] S. Yang, C.-H. Lee, and C.-C. J. Kuo, "Optimized mesh and texture multiplexing for progressive textured model transmission," 2004, p. 676–683.
- [27] F. Caillaud, V. Vidal, F. Dupont, and G. Lavoué, "Progressive compression of arbitrary textured meshes," *Computer Graphics Forum*, vol. 35, no. 7, pp. 475–484, 2016.
- [28] Z. Wang, E. Simoncelli, and A. Bovik, "Multiscale structural similarity for image quality assessment," in *Asilomar Conference on Signals, Systems Computers*, vol. 2, 2003, pp. 1398–1402 Vol.2.
- [29] L. Zhang, L. Zhang, X. Mou, and D. Zhang, "Fsim: A feature similarity index for image quality assessment," *IEEE Transactions on Image Processing*, vol. 20, no. 8, pp. 2378–2386, 2011.
- [30] H. Sheikh and A. Bovik, "Image information and visual quality," *IEEE Transactions on Image Processing*, vol. 15, no. 2, pp. 430–444, 2006.
- [31] A. Mittal, A. K. Moorthy, and A. C. Bovik, "No-reference image quality assessment in the spatial domain," *IEEE Transactions on Image Processing*, vol. 21, no. 12, pp. 4695–4708, 2012.
- [32] E. M. Torlig, E. Alexiou, T. A. Fonseca, R. L. de Queiroz, and T. Ebrahimi, "A novel methodology for quality assessment of voxelized point clouds," in *Applications of Digital Image Processing XLI*, vol. 10752. International Society for Optics and Photonics, pp. 174 – 190.
- [33] A. K. Moorthy and A. C. Bovik, "Blind image quality assessment: From natural scene statistics to perceptual quality," *IEEE Transactions on Image Processing*, vol. 20, no. 12, pp. 3350–3364, 2011.
- [34] "Modified-brisque as no reference image quality assessment for structural mr images," *Magnetic Resonance Imaging*, vol. 43, pp. 74–87, 2017.
- [35] Q. Méricot, M. Ovsjanikov, and L. J. Guibas, "Voronoi-based curvature and feature estimation from point clouds," *IEEE Transactions on Visualization and Computer Graphics*, vol. 17, no. 6, pp. 743–756, 2011.
- [36] T. Surazhsky, E. Magid, O. Soldea, G. Elber, and E. Rivlin, "A comparison of gaussian and mean curvatures estimation methods on triangular meshes," in *IEEE International Conference on Robotics and Automation*, vol. 1, 2003, pp. 1021–1026 vol.1.
- [37] P. Alliez, D. Cohen-Steiner, O. Devillers, B. Lévy, and M. Desbrun, "Anisotropic polygonal remeshing," 2003.
- [38] M. Corsini, E. D. Gelasca, T. Ebrahimi, and M. Barni, "Watermarked 3-d mesh quality assessment," *IEEE Transactions on Multimedia*, vol. 9, no. 2, pp. 247–256, 2007.
- [39] N. Mukherjee, "A hybrid, variational 3d smoother for orphaned shell meshes," in *IMR*, 2002.
- [40] H. Lee, P. Alliez, and M. Desbrun, "Angle-analyzer: A triangle-quad mesh codec," *Computer Graphics Forum*, vol. 21, no. 3, pp. 383–392.
- [41] I. Abouelaziz, M. El Hassouni, and H. Cherifi, "No-reference 3d mesh quality assessment based on dihedral angles model and support vector regression," in *Image and Signal Processing*, Cham, 2016, pp. 369–377.
- [42] "Scikit-learn for python." [Online]. Available: <https://scikit-learn.org/stable/>
- [43] Z. Wang and Q. Li, "Information content weighting for perceptual image quality assessment," *IEEE Transactions on Image Processing*, vol. 20, no. 5, pp. 1185–1198, 2011.
- [44] A. Mittal, R. Soundararajan, and A. C. Bovik, "Making a "completely blind" image quality analyzer," *IEEE Signal Processing Letters*, vol. 20, no. 3, pp. 209–212, 2013.
- [45] I. Abouelaziz, M. El Hassouni, and H. Cherifi, "A curvature based method for blind mesh visual quality assessment using a general regression neural network," in *International Conference on Signal-Image Technology and Internet-Based Systems*, 2016, pp. 793–797.
- [46] H. Sheikh, M. Sabir, and A. Bovik, "A statistical evaluation of recent full reference image quality assessment algorithms," *IEEE Transactions on Image Processing*, vol. 15, no. 11, pp. 3440–3451, 2006.